JOURNAL OF CATALYSIS 150, 155–169 (1994)

HDS Activity and Characterization of Zeolite-Supported Nickel Sulfide Catalysts

W. J. J. Welters, G. Vorbeck, H. W. Zandbergen,* J. W. de Haan, V. H. J. de Beer, and R. A. van Santen

*Schuit Institute of Catalysis, Eindhoven University of Technology, P.O. Box 513, 5600 MB Eindhoven, The Netherlands; and *Center for High Resolution Electron Microscopy, Delft University of Technology, Rotterdamseweg 137, 2628 AL Delft, The Netherlands*

Received November 8, 1993; revised April 15, 1994

Catalysts of nickel sulfide supported on zeolite Y have been prepared (by impregnation or ion exchange) and characterized by means of thiophene hydrodesulfurization (HDS), sulfur analysis, temperature-programmed sulfiding, ^{129}Xe-NMR, HREM and dynamic oxygen chemisorption. The catalysts show large differences in catalytic behavior dependent on the preparation method (impregnation vs ion exchange) and the pretreatment conditions (method of sulfidation). Especially the ion-exchanged catalysts show a high initial activity, but due to the presence of acid sites deactivation is very strong. The initial activity of these catalysts can be improved significantly by drying prior to sulfidation. In all cases sulfidation results in quantitative formation of nickel sulfide, with Ni_3S_2 being the main product. Occasionally, also some NiS appears to be present. The major part of the nickel sulfide phase is invariably located on the outside of the zeolite particles. The fraction of nickel sulfide in the zeolite pores depends on the preparation method and the pretreatment conditions. The differences in catalytic activity are ascribed not only to variations in overall nickel sulfide dispersion but also to the acidity of the support, and the presence of very active small nickel sulfide clusters in the pores of the zeolite can have a strong influence on the thiophene HDS activity.

INTRODUCTION

Hydrocracking is one of the major catalytic processes to convert residual feedstocks into distillate products. A hydrocracking catalyst needs both an acid and a hydrogenation function. In industrial hydrocracking processes combinations of zeolites and transition metal sulfides are often used. These catalysts are more active than metal sulfides on silica-alumina, yield more desirable products (light hydrocarbons and gasolines) and are more resistant to poisoning by sulfur and nitrogen-containing compounds present in the feed (1, 2). For process economics the availability of catalysts having an activity and selectivity adapted to the feed requirements is of crucial importance. However, the selection of these tailor-made catalysts is still difficult because of the limited knowledge about the influence of parameters such as the location of the sulfide species (in- or outside of the zeolite pore system), the interaction between sulfide species and the zeolite and their effect on the catalytic activity.

Several studies about zeolite-supported transition metal sulfides have been reported in recent years (3–11). Cid *et al.* (3, 4) found zeolite-supported cobalt sulfide catalysts prepared by ion exchange to be more active for thiophene hydrodesulfurization (HDS) than those prepared by impregnation. Sulfided ion exchanged NiNaY zeolites showed an increase in steady state thiophene HDS activity with increasing Ni loading. Sulfidation led to the formation of nickel sulfide (probably Ni_3S_2), accompanied by an increase in Brønsted acidity (6). Leglise *et al.* (10) and Ezzamarty *et al.* (11) studied sulfided Ni and Ni–Mo catalysts supported on dealuminated Y zeolites. They found incomplete sulfidation for all the Ni–Mo catalysts, but the Ni catalysts sulfided well. From XPS analysis they concluded that in the oxidized state Ni concentrated near the zeolite surface (ion exchange) and that it became better dispersed upon sulfidation. Welters *et al.* (12) compared zeolite Y supported Ni and Co sulfide catalysts with the corresponding ones supported on Al_2O_3 and carbon. Both metal sulfides had similar activities which were considerably higher than those of their alumina-supported counterparts, and comparable to that of carbon-supported catalysts.

In the present study zeolite Y-supported nickel sulfide catalysts have been prepared by impregnation and ion exchange. In spite of the fact that stabilized Y zeolites are the most commonly used zeolites for industrial hydrocracking (1), the original Y zeolite has been used as support for our model catalysts in order to avoid activity changes arising from the extra-framework alumina or from the voids or lattice defects present in the stabilized Y zeolite. Thiophene HDS at atmospheric pressure has been used as test reaction. Although this reaction does not provide direct information about the hydrocracking properties of the catalysts, it is a relatively short and useful

0021-9517/94 $6.00

test for first stage comparison of the activities of catalyst series. Several other techniques have been used to characterize the catalysts, for instance the acidity of the zeolite has been studied by ethylamine TPD, the nickel sulfide phase by sulfur analysis and temperature-programmed sulfiding (TPS) and the distribution of the sulfide species throughout the zeolite particles by ^{129}Xe-NMR, HREM and O_2 chemisorption.

EXPERIMENTAL

Catalyst Preparation

A series of NiNaY catalysts with varying degrees of ion exchange were prepared at room temperature from a NaY zeolite (PQ CBV-100, $Na_{54}(AlO_2)_{54}(SiO_2)_{138} \cdot x\ H_2O$) using aqueous solutions of $NiCl_2$ of appropriate concentrations. After exchange the samples are washed until Cl^- free, and dried in air at 383 K for 16 h. A CaY zeolite ($Ca_{25}Na_4(AlO_2)_{54}(SiO_2)_{138} \cdot x\ H_2O$) was prepared from the NaY zeolite by repeated ion exchange with $CaCl_2$ aqueous solutions. The metal contents of the exchanged zeolites were determined using atomic absorption spectroscopy (AAS). Two series of catalysts were prepared by pore volume impregnation of NaY and CaY zeolites with aqueous solutions of $Ni(NO_3)_2$. After impregnation the samples were dried in air overnight at 383 K, and subsequently calcined at 673 K for 2 h. All samples were stored in a desiccator over a saturated $CaCl_2$ solution. The catalysts are designated Ni(x)NaY (ionex), Ni(x)/NaY (imp), or Ni(x)/CaY (imp), with x representing the weight percentage Ni (determined by AAS and calculated on the basis of the water free zeolite).

Catalytic Activity

Thiophene hydrodesulfurization (HDS) activity measurements were carried out in a flow microreactor under standard conditions (673 K, 1 atm, 4.0% thiophene in H_2, 50 std cm^3 min^{-1}). Catalyst samples of 0.25 g (particle size 0.125–0.425 mm) were sulfided *in situ* using a mixture of 10% H_2S in H_2 (60 std cm^3 min^{-1}, 6 K min^{-1} from 293 K to 673 K, 2 h at 673 K). In some cases sulfidation was preceded by *in situ* drying at 673 K (heating rate 6 K min^{-1}) in a He flow. These catalysts will be referred to as Ni(x)NaY (ionex, dry sulf).

After sulfidation the flow was switched to the thiophene/H_2 flow. Reaction products were analyzed by on-line GC analysis. The first sample was taken after 2 min reaction time and the following ones at intervals of 35 minutes. Due to the presence of acid sites, considerable polymerization (unsaturated products), and cracking (butenes and polymerized products) took place, resulting in a large variety of products and coke formation. Therefore, thiophene converted to any of the reaction products including coke was taken into account for the calculation of the reaction rate constant (k_{HDS}) assuming the reaction to be first order in thiophene (13). Coke formation which often causes strong deactivation due to shielding of the metal sulfide phase can severely hamper the evaluation of the intrinsic catalytic properties. Therefore, we compared the catalysts also on the basis of their activity at very short run time (2 min).

Structure and Composition

The coke content of deactivated catalyst samples was analyzed via oxidation in a O_2/He flow (20% O_2), and by measuring the weight loss by thermogravimetric analysis (TGA) using a Setaram TG 85-16-18 balance. The products were qualitatively analyzed by *in situ* mass spectrometry (Leybold Quadruvac PGA100). Because the oxidation of the coke deposits and the metal sulfide cannot be separated, the measured weight loss was corrected for the weight loss due to oxidation of the nickel sulfide, assuming a composition as determined by the sulfur analysis.

The number of acid sites present after sulfidation was determined by temperature programmed desorption (TPD) of ethylamine (14, 15). Ethylamine was adsorbed on the *in situ* dried sample (673 K in He flow) until full saturation. After adsorption, first an isothermal desorption of ethylamine was carried out at 323 K, and then the TPD procedure was started. During TPD the weight loss was again measured by TGA, while the desorbed products were identified by mass spectrometry. The physisorbed ethylamine will desorb in the temperature range between 323 K and 600 K, while the ethylamine adsorbed on Brønsted acid sites only desorbs after decomposition to NH_3 and C_2H_4 between 650 K and 750 K (14, 15). From the weight loss at high temperature the amount of ethylamine adsorbed on Brønsted acid sites could be calculated. This amount is a good indication for the number of Brønsted acid sites.

The total sulfur uptake during sulfidation was determined as follows. A sample was dissolved in aqua regia while carefully heating the mixture. During this process the nickel sulfide was completely converted to nickel sulfate. Subsequently, the amount of sulfate was determined by titration with barium perchlorate. Ca^{2+} ions disturb the titration and must be removed from the solution by an ion exchanger. Before analysis the catalyst was sulfided using the same procedures as for the catalytic activity measurements. After sulfidation the sample was flushed with He at 673 K for 1 h to remove adsorbed H_2S and subsequently cooled down under He. At room temperature the sample was exposed to air, and the analysis procedure was started.

The sulfidation behavior of the catalysts was studied in more detail by temperature programmed sulfidation

(TPS). A detailed description of this technique has been given elsewhere (16, 17). A flow of $H_2S/H_2/Ar$ was passed over a catalyst sample loaded in a quartz tube which was placed in an oven. The H_2S concentration in the reactor outlet was measured by a UV spectrophotometer (at 195 nm). After H_2O and H_2S were trapped using molecular sieves and ZnO, respectively, the gases were led through a thermal conductivity detector where changes in the H_2 concentration were monitored. A sulfiding mixture of 3.3% H_2S, 28.1% H_2, and 68.6% Ar with a flow of 40 std $cm^3\ min^{-1}$ was used. The measurements were carried out according to the following procedure. The reactor was flushed with argon in order to remove air, followed by sulfidation at room temperature for 10 min. Then the reactor temperature was raised at 6 K min^{-1} up to 673 K. This temperature was maintained for 1 h, followed by further heating at 10 K min^{-1} up to 1273 K.

^{129}Xe-NMR was used to study the amount of nickel sulfide located inside the zeolite pore system. The principle and experimental details of this technique are reported elsewhere (18–20). To avoid contact with O_2 and H_2O the presulfided samples were transferred into the NMR tubes using a recirculation type glove box (O_2 and H_2O content lower than 2 ppm). The samples were evacuated at room temperature to a pressure below 10^{-4} mbar and stored in a volumetric adsorption apparatus. Xe was adsorbed on these samples at different Xe pressures at 303 K. The NMR spectra of the adsorbed Xe were recorded at the same temperature on a Bruker MSL 400 Fourier transform instrument at 110.7 MHz with pulse excitation (0.5 s pulse delay) on stationary samples. The number of scans varied between 10^2 and 10^5.

To study the amount of nickel phase formed at the exterior of the zeolite particles high resolution electron microscopy (HREM) was performed on both oxidic and sulfided samples, using a Philips CM 30 ST electron microscope. The samples were prepared as follows. After grinding, the Ni-containing zeolite particles were suspended in alcohol. A copper grid coated with a microgrid carbon polymer was loaded with a few droplets of this suspension. Together with HREM, the transition metal distribution throughout the catalyst particles could be studied (integrally or segment-wise) by means of Energy Dispersive X-ray (EDX) analysis.

Dynamic oxygen chemisorption (DOC) measurements were used to determine the relative nickel sulfide dispersions (21–24). For this purpose catalysts were sulfided *in situ* following the same procedures as for the activity measurements. After sulfidation, the catalysts (about 100 mg) were flushed for 1 hour at 673 K in He (O_2 and H_2O levels lower than 1 ppm), and then cooled to 333 K, at which temperature the oxygen chemisorption was performed. At this temperature the support has no effect on the oxygen chemisorption. According to Bachelier *et al.* (21–23), side reactions (SO_2 and COS formation) are avoided, and the oxygen is chemisorbed irreversibly on the sulfide catalyst. Pulses of a 5% O_2 in He were injected into the He carrier gas flow and passed over the catalyst and a thermocouple detector. When effluent peaks had increased to constant size (less than 1% difference between two successive peaks) the total O_2 uptake was calculated.

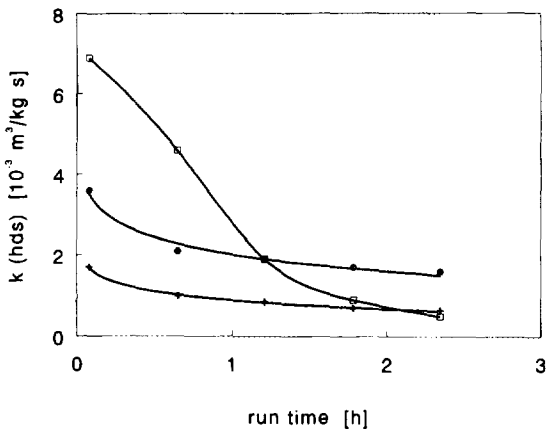

FIG. 1. Thiophene HDS activity versus run time, for different zeolite Y-supported nickel sulfide catalysts: +, Ni(4)/NaY (imp); ●, Ni(4)/CaY (imp); □, Ni(4)NaY (ionex).

RESULTS

Thiophene HDS

As can be seen from Fig. 1, the behavior of sulfided zeolite Y-supported Ni catalysts during the thiophene HDS reaction clearly depends on the preparation method used. Of the two impregnated catalysts, Ni(4)/CaY (imp) has a higher activity than the Ni(4)/NaY (imp) and also its deactivation is somewhat stronger. Initially, the ion exchanged catalyst has a high thiophene HDS activity but due to a very strong deactivation its activity is very low after 2 h run time.

The deactivation is at least partially caused by the high amount of coke which is formed on all catalysts during reaction. The amounts of coke deposited on the catalysts after 3 h run time are given in Table 1. These data are obtained by measuring the weight loss during temperature programmed oxidation (TPO). Since the TPO products are analyzed by mass spectrometry the weight loss can be ascribed to oxidation of carbon to CO_2 and small quantities of sulfur (SO_2 and SO_3 products). The latter can arise from sulfur-containing coke products as well as the nickel sulfide phase which is present in these catalysts. These results indicate that the coke deposits are probably formed by polymerization of the sulfur-free reaction prod-

TABLE 1

Initial (at 2-Min Run Time) Product Selectivities (mol/mol) of Zeolite Y-Supported Nickel Sulfide Catalysts (4 wt% Ni) and the Amount of Coke Deposited after 3 h

Products	Ni(4)/NaY (imp)	Ni(4)/CaY (imp)	Ni(4)NaY (ionex)
C_1–C_3	9	23	32
C_4	76	52	36
$>C_4$	15	25	32
coke [wt%]	7	12	20

ucts, and not directly from the thiophene itself (in this case more S would have been present in the coke deposits). The amount of coke on the catalysts increases with increasing activity, but also with increasing acidity of the zeolite support. In addition, BET measurements showed that the micropore volume of Ni(4)NaY (ionex) is strongly reduced during the catalytic measurement (0.32 $cm^3\ g^{-1}$ for the freshly sulfided zeolite and 0.02 $cm^3\ g^{-1}$ after 3 h thiophene HDS). Therefore, we can conclude that the very strong deactivation of this catalyst is caused to a large extent by coke formation.

Also the product distribution clearly varies with the type of catalyst. In Table 1 one can see that the C_4 product selectivity (butanes and butenes; butadiene is not formed in detectable amounts) decreases in the order Ni(4)/NaY (imp) > Ni(4)/CaY (imp) > Ni(4)NaY (ionex). The C_4 products mainly consist of *n*-butane and the *n*-butenes, but especially on the more acidic catalysts also small amounts of isobutane are present. The latter are probably formed during cracking of polymerized products. Besides C_4 products, also products resulting from cracking (C_1–C_3) and polymerization reactions ($>C_4$) are detected. These secondary reactions, including coke formation, most probably take place on acid sites since they depend strongly on the acidity of the sulfided catalysts.

Several methods can be used to measure the acidity of zeolitic catalysts (25, 26). A convenient way to measure the number of acid sites is by ethylamine desorption (14, 15). The results of these measurements are given in Table 2. The pure NaY support showed no desorption of ethylamine around 700 K which is to be expected as NaY does not contain any Brønsted acid sites. The results show that the sulfided Ni(4)/NaY (imp) catalyst is slightly acidic. There can be several reasons for this. The presence of nickel sulfide might cause some acidity. However, a sulfidic Ni/Al_2O_3 catalyst desorbs hardly any ethylamine in the temperature range between 650 K and 750 K, meaning that there are no Brønsted acid sites present on the nickel sulfide phase in this catalyst. Hence, probably the acidity of the Ni(4)/NaY (imp) is not caused by the nickel sulfide. Another possibility for the generation of acid sites is the replacement of some Na^+ ions by Ni^{2+} ions via ion exchange that might take place during impregnation. The Na^+ ions remain on the zeolite and will form small NaCl crystals upon drying. After sulfidation the Ni^{2+} ions are converted into nickel sulfide, and their position in the zeolite lattice is probably taken by protons resulting in a somewhat acidic catalyst.

Ni(4)/CaY (imp) shows a much higher acidity, due to the formation of acid sites by protolysis of the water molecules adsorbed on the Ca^{2+} ions. Also the sulfided Ni(4)NaY (ionex) shows a high number of acid sites probably formed during sulfidation of the Ni^{2+} ions as described above. Complete replacement of Ni^{2+} by protons would have resulted in 1.06 mmol g^{-1} Brønsted acid sites. However, the ethylamine desorption experiments usually give results which are somewhat lower than the theoretical values (14, 15). Moreover, it might also be that after sulfidation some of the acid sites cannot be reached by ethylamine because they are blocked by nickel sulfide particles formed in the zeolite pores.

The acidity difference between Ni(4)/NaY (imp) and Ni(4)/CaY (imp) agrees well with the observed coking behavior and their product selectivities. However, Ni(4)/CaY (imp) and Ni(4)NaY (ionex) have almost the same number of acid sites, although their coking behavior and product selectivities are quite different.

In addition to coking also sintering of the nickel sulfide phase can influence the catalyst deactivation. It was thought that oxidation (at 773 K in static air for 2 h) and resulfidation of a deactivated catalyst, followed by an activity measurement, might provide more insight into this matter. As shown in Fig. 2, oxidation and resulfidation of a freshly sulfided Ni(4)NaY (ionex) catalyst results in a small drop of the initial activity (which is taken as a characteristic for the activity of the metal sulfide phase, because at higher run time deactivation due to coking will have taken place), probably caused by a small loss of dispersion during these two additional pretreatments. Oxidation and resulfidation of the deactivated ion-exchanged

TABLE 2

The Acidity of Zeolite Y-Supported Nickel Sulfide Catalysts as Measured by Ethylamine Desorption between 575 K and 725 K

Catalyst	Ethylamine desorption [mmol/g catalyst]
Ni(4)/NaY (imp)	0.27
Ni(4)/CaY (imp)	0.83
Ni(4)NaY (ionex)	0.80

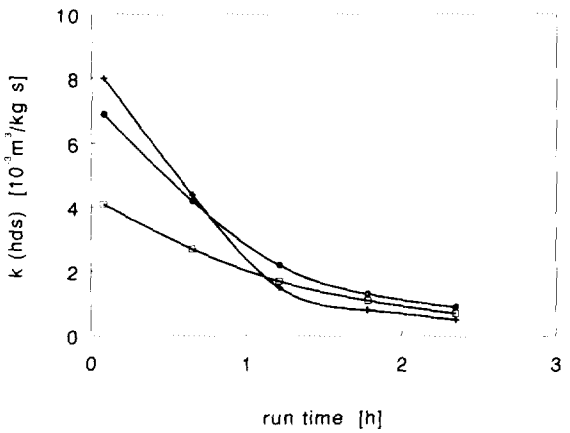

FIG. 2. Thiophene HDS activity versus run time for oxidized and resulfided Ni(4)NaY (ionex) catalysts: +, standard sulfidation; ●, sulfided, oxidized, and resulfided sample; □, sulfided, 3 h thiophene HDS, oxidized, and resulfided sample.

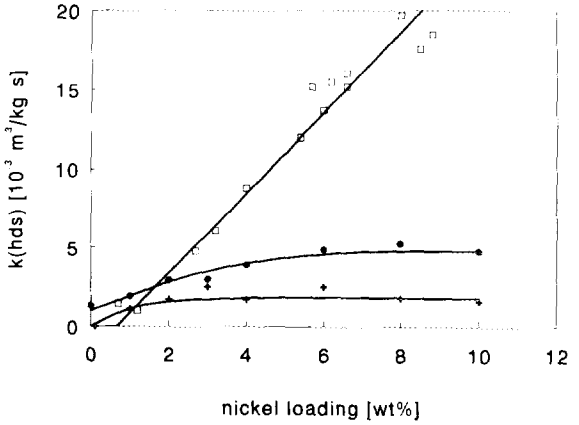

FIG. 3. Initial thiophene HDS activity (at 2 min run time) versus nickel loading for series of differently prepared zeolite Y-supported nickel sulfide catalysts: +, Ni(x)/NaY (imp); ●, Ni(x)/CaY (imp); □, Ni(x)NaY (ionex).

catalyst results in a lower initial activity, indicating that during thiophene HDS sintering of the nickel sulfide particles occurs. However, part of the observed activity decrease might be due to sintering caused by carbonaceous residue burn-off during oxidation of the spent catalyst. On the other hand, it is also very well possible that during oxidation a fraction of the Ni ions is redistributed over the zeolite by reoccupying the cation positions in the ion-exchanged zeolite structure, thus causing the reverse effect of sintering. After resulfidation these Ni ions will give the same nickel sulfide dispersion as for the freshly sulfided catalyst. Hence, probably some of the deactivation of the Ni(4)NaY (ionex) is caused by sintering of the nickel sulfide phase, but from the oxidation experiments the extent of this effect cannot readily be estimated.

As can be seen from Fig. 3, the three different types of catalyst also develop different initial HDS activity patterns when the nickel loading is gradually increased. At low loadings both the Ni(x)/NaY (imp) and the Ni(x)/CaY (imp) show an activity increase with increasing Ni content, but at higher loadings the activity remains constant. In clear contrast herewith, the initial activity of the Ni(x)NaY (ionex) catalysts increases linearly with increasing Ni content. Especially at relatively high Ni loadings this results in catalysts having a very high initial activity, which however deactivate very rapidly.

In their oxidic state all zeolite Y supported catalysts contain a high amount of adsorbed water (up to 25 wt%). In order to examine its influence, the catalysts were dried in a He stream at 673 K prior to sulfidation. After drying two procedures were followed: (I) cooling to room temperature and standard sulfidation, (II) direct sulfidation at 673 K. In the second procedure the water formed during the sulfidation reaction cannot adsorb on the zeolite, but will immediately be removed by the H_2S/H_2 gas flow. In this way the effect of the water on the sulfidation of the catalyst will be minimalized. However, both these procedures give the same thiophene HDS results. For the ion-exchanged catalysts the initial activity increases markedly (see Fig. 4) compared to the standard sulfidation. This increase is the strongest at low metal loadings (see Fig. 5). At higher metal loadings (6 and 8 wt% Ni) the k_{HDS} seems to remain constant around a value of about 23×10^{-3} m^3 kg^{-1} s^{-1}. Possibly for these catalysts the reaction rate is influenced by pore diffusion limitations, but it might also be that the nickel sulfide surface area has reached a maximum at these metal loadings. In the case of the impregnated catalysts the influence of these pretreatments

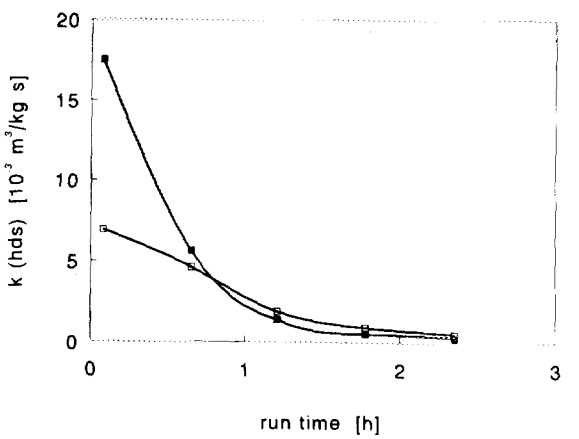

FIG. 4. Thiophene HDS activity versus run time for differently sulfided Ni(4)NaY (ionex) catalysts: □, standard sulfidation (6 K min^{-1} to 673 K and 2 h at 673 K in 10% H_2S in H_2); ■, dried before sulfidation (6 K/min to 673 K in He, at 673 K 10% H_2S in H_2 for 2 h).

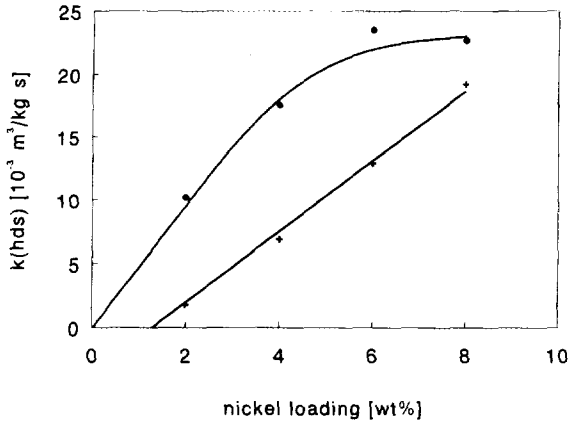

FIG. 5. Initial thiophene HDS activity versus nickel loading on Ni(x)NaY (ionex) zeolites for different sulfidation pretreatments: +, standard sulfidation; ●, dried before sulfidation (conditions: see Fig. 4).

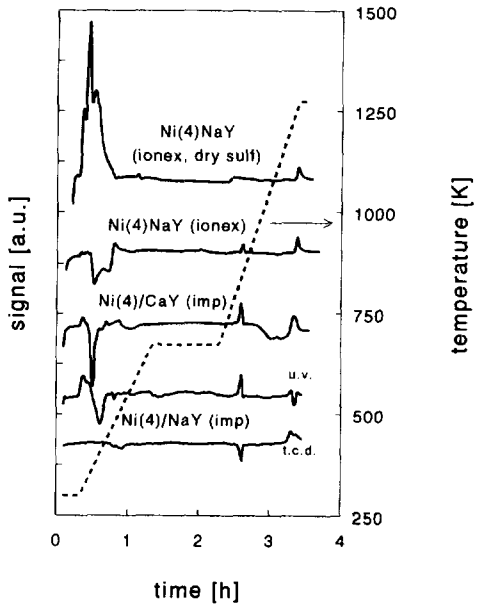

FIG. 6. TPS patterns recorded for various zeolite Y-supported nickel catalysts. A negative peak means consumption of H_2S or H_2, a positive peak means desorption.

on the initial activity is far less strong, and for Ni(x)/NaY (imp) it is even negligible.

Overall Sulfur Analysis and TPS

The sulfidation behavior of the catalysts was analyzed with TPS and overall sulfur analysis. The results of the latter method are given in Table 3. From this we can conclude that all catalysts sulfide well, with Ni_3S_2 being the most probable nickel sulfide phase. XRD experiments revealed that the crystallinity of the zeolite support is not changed during preparation nor during sulfidation.

The TPS patterns presented in Fig. 6 show that for the standard sulfidation procedure there are only minor differences in sulfidation behavior between the three types of catalyst. All catalysts sulfide at temperatures below 550 K. Both impregnated catalysts show at first some desorption of H_2S which had been adsorbed during the isothermal period at 293 K. Around 375 K a large consumption of H_2S is seen, indicating that sulfidation of the nickel takes place. The NaY and CaY supports do not show any detectable H_2S or H_2 consumption at temperatures below 673 K. The Ni(4)NaY (ionex) catalyst gives a slightly different pattern compared to the impregnated catalysts. Again, the sulfidation of the Ni species starts around 375 K, but now a slightly higher temperature is needed to complete the sulfidation process. Perhaps some Ni ions, for instance those present in the hexagonal prisms of zeolite Y, are sulfided less easily. For all catalysts a small consumption of H_2 (only shown for Ni(4)/NaY (imp)) accompanied by some H_2S production can be seen around 500 K. These are due to reduction of elemental S formed during the sulfidation reaction (16):

$$3NiO + 3H_2S \rightarrow Ni_3S_2 + 3H_2O + S.$$

Possibly also some NiS has been formed during sulfidation (this would explain the somewhat higher Ni : S ratio in Table 3 compared with Ni_3S_2). Unfortunately, a quantitative analysis of the amounts of H_2S and H_2 consumed during sulfidation cannot be made due to baseline instabilities of the UV and TCD detectors. Therefore, it is not possible to calculate a Ni : S ratio based on the TPS experiments.

If the Ni(4)NaY (ionex) zeolite is dried at 673 K in He before sulfidation a completely different TPS profile is obtained. The H_2S adsorption during the isothermal period at 293 K has strongly increased. This may be due to adsorption of H_2S on the zeolite support. The very large amount of H_2S adsorbed during the isothermal period desorbs as the catalyst is heated. As a consequence, no further H_2S consumption can be measured during heating. The catalyst is sulfided somewhere between 293 K and

TABLE 3

Overall Sulfur Analysis of Zeolite Y-Supported Nickel Sulfide Catalysts

Catalyst	Ni : S ratio
Ni(4)/NaY (imp)	3 : 2.2
Ni(4)/CaY (imp)	3 : 2.1
Ni(4)NaY (ionex)	3 : 2.1
Ni(4)NaY (ionex, dry sulf)	3 : 2.0

550 K probably using the H_2S adsorbed previously at 293 K. The strong color change from slightly pink to dark grey during the H_2S adsorption at 293 K might indicate that sulfidation at least to some extent takes place at room temperature. For the catalysts not dried in He before sulfidation the color change at room temperature is far less strong (both the impregnated catalysts become slightly more grey than they are in the oxidic phase, while the Ni(4)NaY (ionex) changed from light green into light grey). The fact that for all catalysts sulfidation is already complete at 550 K (above this temperature no significant H_2S consumption is observed) indicates that unlike in the case of Ni/Al_2O_3 there is no strong interaction between the support and the nickel phase which could hamper sulfidation of nickel species (17).

All catalysts except the Ni(4)NaY (ionex, dry sulf) show H_2S production at 810 K, accompanied by H_2 consumption. The amounts of H_2S produced are rather small, about 10% of all the H_2S consumed during sulfidation for the impregnated catalysts, and clearly less for the ion-exchanged catalyst. According to Scheffer *et al.* (17) this peak is caused by the NiS to Ni_3S_2 phase transition. Overall sulfur analysis of the catalysts showed that after standard sulfidation at 673 K the amount of sulfur present is somewhat larger than that required for quantitative Ni_3S_2 formation. This points to the presence of both Ni_3S_2 and NiS.

Around 1250 K all catalysts show small H_2S and H_2 desorption peaks. At this temperature the zeolite framework collapses, during which some small amounts of adsorbed H_2S and H_2 are released. The Ni(4)/CaY (imp) shows H_2S adsorption between 1000 and 1250 K, caused by the sulfidation of the CaY zeolite.

^{129}Xe NMR

One of the main questions in the preparation of zeolite-supported nickel sulfide catalysts is whether the sulfide species are located inside or outside the zeolite pores. One possibility to confirm the presence of nickel compounds inside the zeolite supercages is to measure the ^{129}Xe nuclear magnetic resonance chemical shifts of Xe adsorbed in the micropores of zeolites along with the Xe adsorption isotherms (18). Series of oxidic and sulfided Ni(x)/NaY (imp) and Ni(x)NaY (ionex) zeolites have already been characterized with these techniques by Korányi *et al.* (20).

In Fig. 7 the Xe adsorption isotherms of a pure NaY zeolite, a Ni(4)NaY (ionex) and a Ni(4)NaY (ionex, dry sulf) are compared. It appears that both sulfided catalysts have an equally lower adsorption capacity than the NaY zeolite, indicating that almost equal amounts of nickel sulfide are located in the zeolite pore system. However, as can be seen in Fig. 8, Ni(4)NaY (ionex, dry sulf) has a larger chemical shift than Ni(4)NaY (ionex). This could

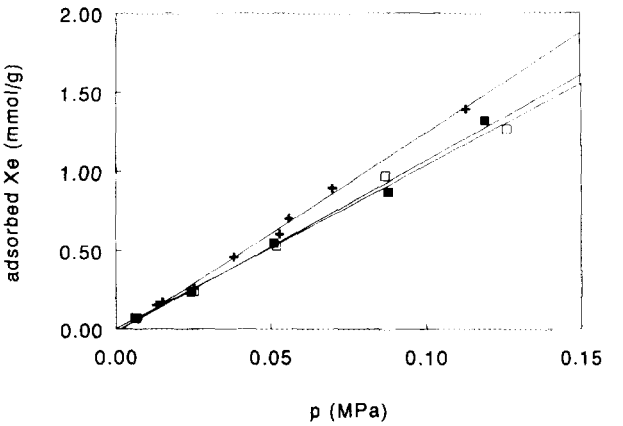

FIG. 7. Xe-adsorption isotherms for sulfided Ni(4)NaY (ionex) and pure NaY: +, NaY; □, standard sulfidation; ■, dry sulfidation (conditions: see Fig. 4).

be the result of a more homogeneous distribution of the nickel sulfide over the zeolite particles, yielding a larger nickel sulfide surface area, which results in a larger interaction of the adsorbed Xe atoms with the nickel sulfide in the pores of the zeolite. Because the chemical shift is influenced by the pore size of the zeolite as well as by the interaction with the substrate (18, 19), it will increase even though the amount of nickel sulfide inside the zeolite pores remains virtually the same.

The increase in chemical shift δ with decreasing Xe concentration (at low Xe adsorption) is most probably also the result of the increased interaction between the Xe atoms and the nickel sulfide. According to the theory of Ito and Fraissard (18, 27) particularly at low Xe pressures each Xe atom will have a relatively long residence time on the nickel sulfide adsorption sites, resulting in an

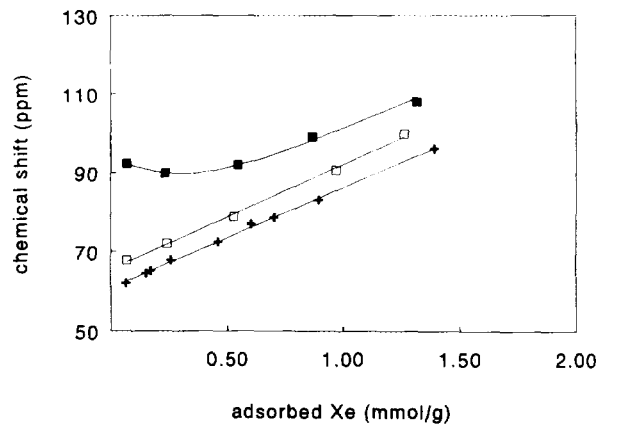

FIG. 8. ^{129}Xe-NMR chemical shift versus the amount of adsorbed Xe for sulfided Ni(4)NaY (ionex) and pure NaY: +, NaY; □, standard sulfidation; ■, dry sulfidation (conditions: see Fig. 4).

increasing δ compared to NaY or to catalysts in which less nickel sulfide surface area is available. When the Xe concentration increases, δ will at first decrease due to the exchange of these adsorbed Xe atoms with those adsorbed on other sites in the NaY zeolite, and then increase with the number of Xe–Xe collisions, as can be seen in Fig. 8 for the Ni(4)NaY (ionex, dry sulf) sample.

HREM and EDX

The distribution of the nickel sulfide over the zeolite particle was also studied by HREM and EDX. The HREM results given in Figs. 9–11 show the presence of large nickel sulfide crystallites (with dimensions up to 50 nm) on the outside of the zeolite particles for all catalysts. In Fig. 9a some very large nickel sulfide crystallites can be observed. They are located on the surface of a zeolite particle which became amorphous due to the high intensity of the electron beam needed for this magnification. The nickel sulfide lattice planes are visible on several crystals. The distances between the lattice fringes (4.9, 2.93, 2.78, and 2.51 Å) agree well with the distances in pure NiS determined by XRD (JCPDS-ICDD 12-41). The number of such large crystalline nickel sulfide particles is, however, very small. Almost all the nickel sulfide on the outside of the zeolite consists of very small adjoining crystallites together forming larger particles, as shown in Fig. 9b. In this figure the nickel sulfide is again located on the outside of an amorphous zeolite particle. The lattice distances (4.87, 2.92, 2.34, and 2.04 Å) which can be measured on the crystalline parts of the nickel sulfide indicate that probably both NiS and Ni_3S_2 are present (JCPDS-ICDD 12-41 and 8-126). A part of the nickel sulfide does not show any lattice fringes, indicating a low crystallinity. This might be due to oxidation of the sulfide phase, because the catalysts are exposed to air during transport from the reactor to the electron microscope.

From HREM results alone, no differences in the sulfide phase distribution over the zeolite particles could be derived for the three different catalysts (Ni(4)/NaY (imp), Ni(4)/CaY (imp) and Ni(4)NaY (ionex)). However, combination with EDX analysis revealed that there are some differences between these catalysts. The average Ni/Si ratio in the EDX spectrum of a great number of zeolite particles is compared with the ratio of a spot on a zeolite particle not containing nickel sulfide at its outer surface. From this comparison an estimate can be made of the relative amounts of nickel sulfide located inside the zeolite pore system. It appeared that for both Ni(4)/NaY (imp) and Ni(4)/CaY (imp) only a small part of the Ni is located inside the zeolite pores (about 20% of the total amount of Ni), while for the Ni(4)NaY (ionex) this amount is only slightly higher (about 30%).

Figure 10 shows a picture of an oxidic Ni(4)/CaY (imp) catalyst before sulfidation. Several zeolite crystals are visible in a crystalline form. At the edges of the crystals dark layers are visible, probably caused by the nickel which after impregnation and calcination is at least partially present as a layer on the outside of the zeolite crystals. Due to the fact that all zeolite particles are almost completely covered by this nickel layer, it is not possible to compare the EDX spectrum of a great number of zeolite particles with that of one zeolite particle not containing nickel sulfide at its outer surface. Consequently no estimation can be made of the percentage of Ni located inside the zeolite pore system.

Figure 11 shows a micrograph of a Ni(4)NaY (ionex, dry sulf) sample. It clearly shows that in this case the nickel sulfide particles are considerably smaller and more numerous. At the surface of the amorphous zeolite small nickel sulfide crystals are visible, but also the dark spots on the amorphous zeolite represent nickel sulfide particle. From the lattice distances it can be concluded that some Ni_3S_2 particles are present. However, other "sulfide" particles cannot be ascribed to either NiS or Ni_3S_2. Possibly these particles have been oxidized to $NiSO_3$ or $NiSO_4$. From EDX measurements on a spot which was free of nickel sulfide particles at the outer surface it can be concluded that the relative amount of nickel which is located inside the zeolite pores is about 40%, which is somewhat higher than for the standard sulfided Ni(4)NaY (ionex).

Dynamic Oxygen Chemisorption (DOC)

The HREM and ^{129}Xe NMR results already revealed that the dispersion of the nickel sulfide phase in the various catalysts studied might differ substantially. Since dispersion is an important parameter influencing the catalytic activity, DOC is used to determine the relative dispersion of the nickel sulfide phase present in the different zeolite supported catalysts. The zeolite support itself (both NaY and CaY) showed no adsorption. In Fig. 12 the oxygen chemisorption is plotted as a function of the metal loading. The Ni(x)/NaY (imp) and Ni(x)/CaY (imp) catalysts appear to have a comparable dispersion at the same metal loading. For both catalysts the nickel sulfide surface area increases with increasing metal loading below 4 wt% Ni. At higher loadings the sulfide surface area does not seem to increase further. At these nickel contents the sulfide surface area of the CaY-supported catalysts seems to be a little higher than that of the NaY-supported catalysts. At Ni loadings below 4 wt% the nickel sulfide dispersion of the Ni(x)NaY (ionex) catalysts is comparable with the impregnated catalysts. However, at higher Ni contents the sulfide surface area continues to increase linearly with increasing metal loading. Drying of the ion-exchanged catalysts before sulfidation enhances the nickel sulfide dispersion. At high loadings the nickel sulfide surface

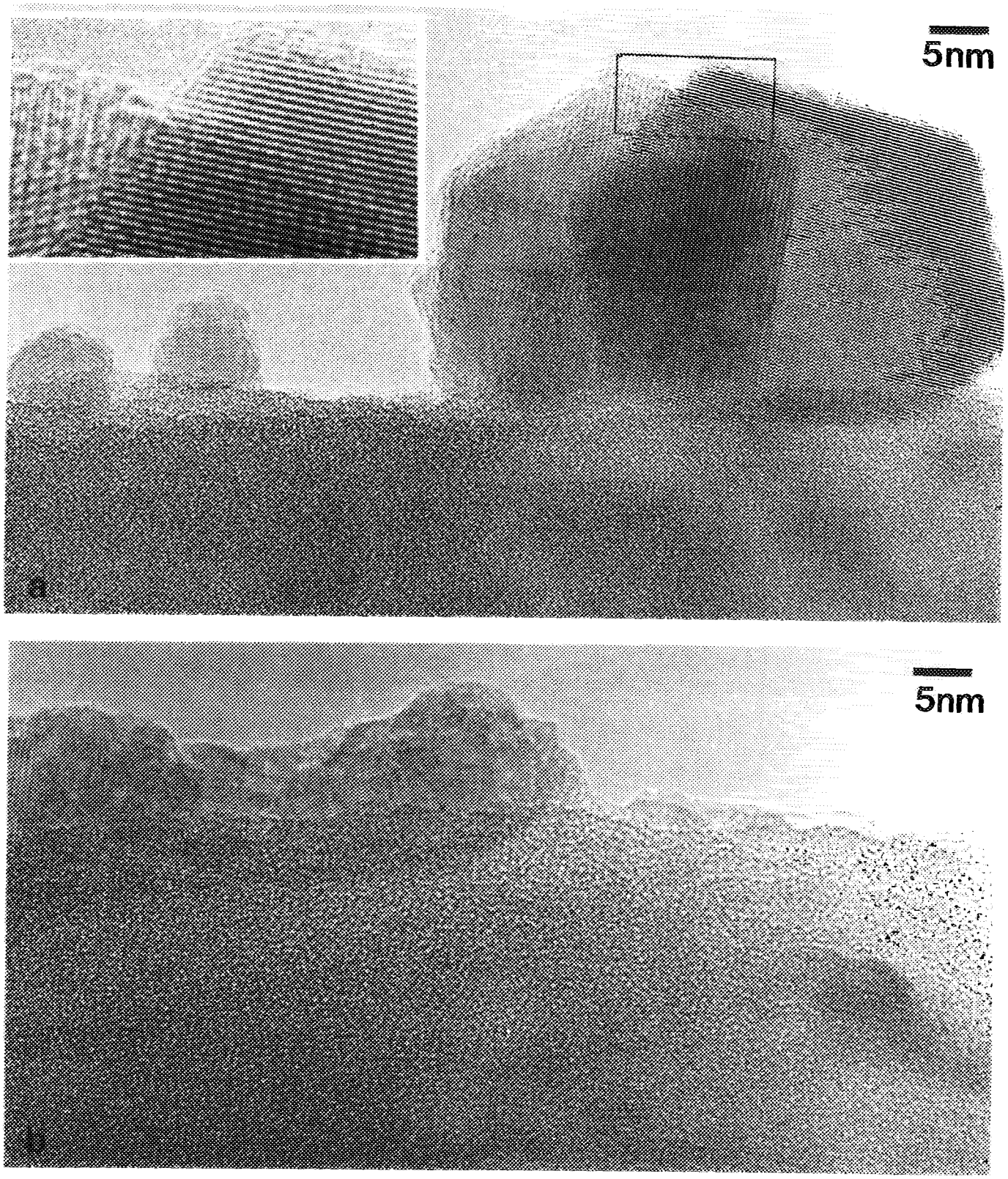

FIG. 9. HREM micrographs of zeolite Y supported nickel sulfide catalysts: (a) Ni(4)NaY (ionex), (b) Ni(4)/CaY (imp).

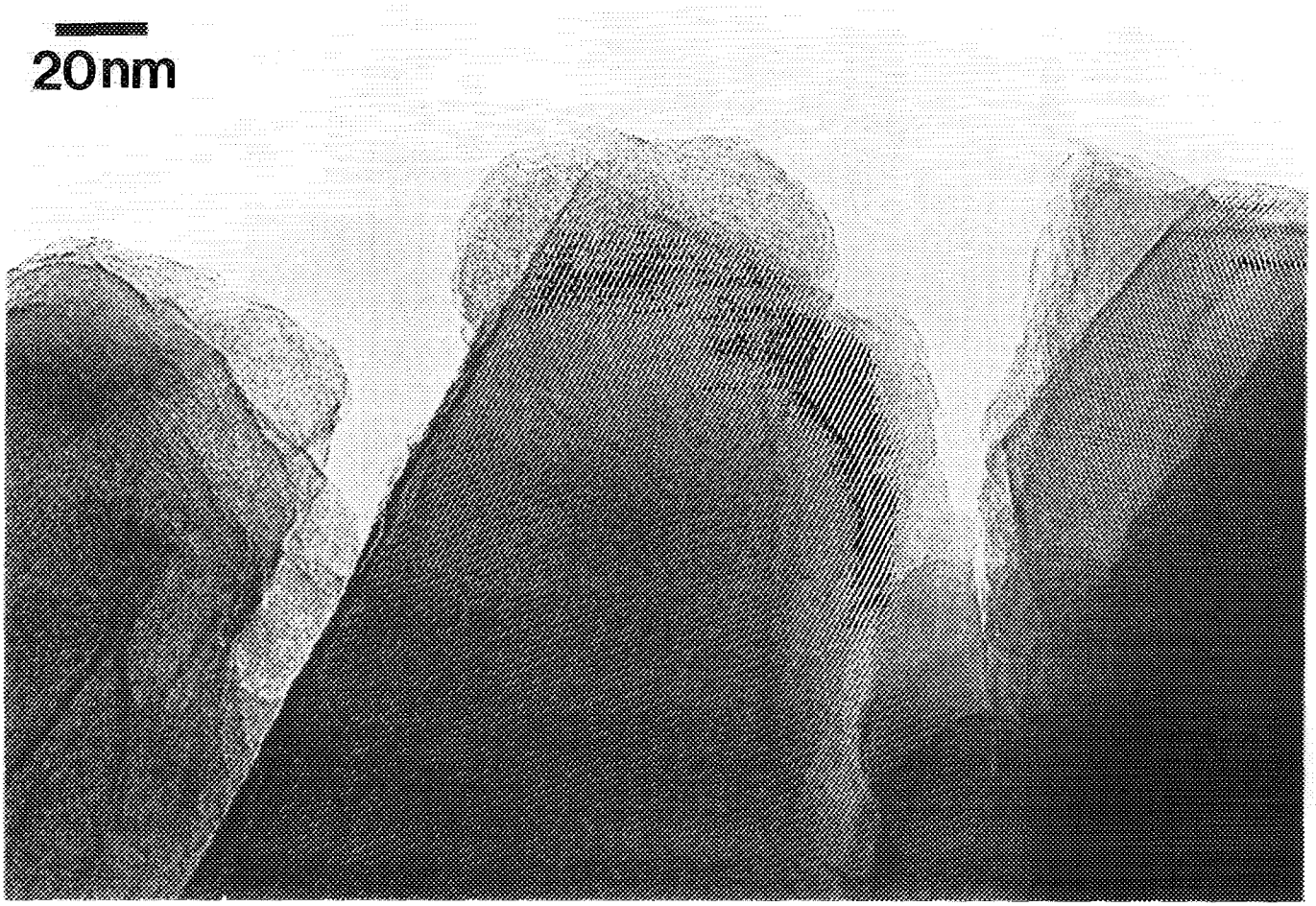

FIG. 10. HREM micrograph of Ni(4)/CaY (imp) before sulfidation.

area of the Ni(x)NaY (ionex, dry sulf) does not increase further. A maximum in the nickel sulfide surface area may have been reached at these high loadings.

DISCUSSION

The observed differences in activity between the various Ni(x)/NaY (imp), Ni(x)/CaY (imp) and Ni(x)NaY (ionex) catalysts and the increase in activity as a result of drying the catalysts before sulfidation may have been caused by variations in nickel sulfide parameters such as (I) type of nickel sulfide, (II) interaction with the zeolite support, (III) distribution (large or small fraction of the nickel sulfide in the pores of the zeolite), or (IV) dispersion. All catalysts were characterized by several techniques in order to examine the influence of these parameters.

Both the TPS experiments and the sulfur analysis show that all catalysts sulfide well. The fact that the sulfidation is completed below 550 K indicates that in the oxidic samples the interaction between the Ni ions and the zeolite framework is rather weak and does not prevent sulfidation, not even for the Ni(4)NaY (ionex) sample in which the Ni^{2+} ions are directly bound to the zeolite framework. The resulting nickel sulfide phase consists mainly of Ni_3S_2, but the TPS experiments (the H_2S desorption around 810 K), the overall sulfur analysis (S/Ni ratio higher than for Ni_3S_2) and also the HREM results (Ni–S lattice distances) indicate that also NiS is present. The HREM results show that the presence of NiS is mainly confined to the large nickel sulfide clusters. In the case of Ni(4)NaY (ionex, dry sulf) which contains hardly any large nickel sulfide clusters (HREM), no reduction of NiS to Ni_3S_2 was observed by TPS, which indicates that this catalyst does not contain NiS. Hence, both the HREM and TPS results suggest that NiS is formed under conditions favoring the generation of large nickel sulfide particles.

For supported catalysts it is unclear which nickel sulfide is thermodynamically the most stable under reaction conditions. For bulk nickel sulfide NiS is thermodynamically

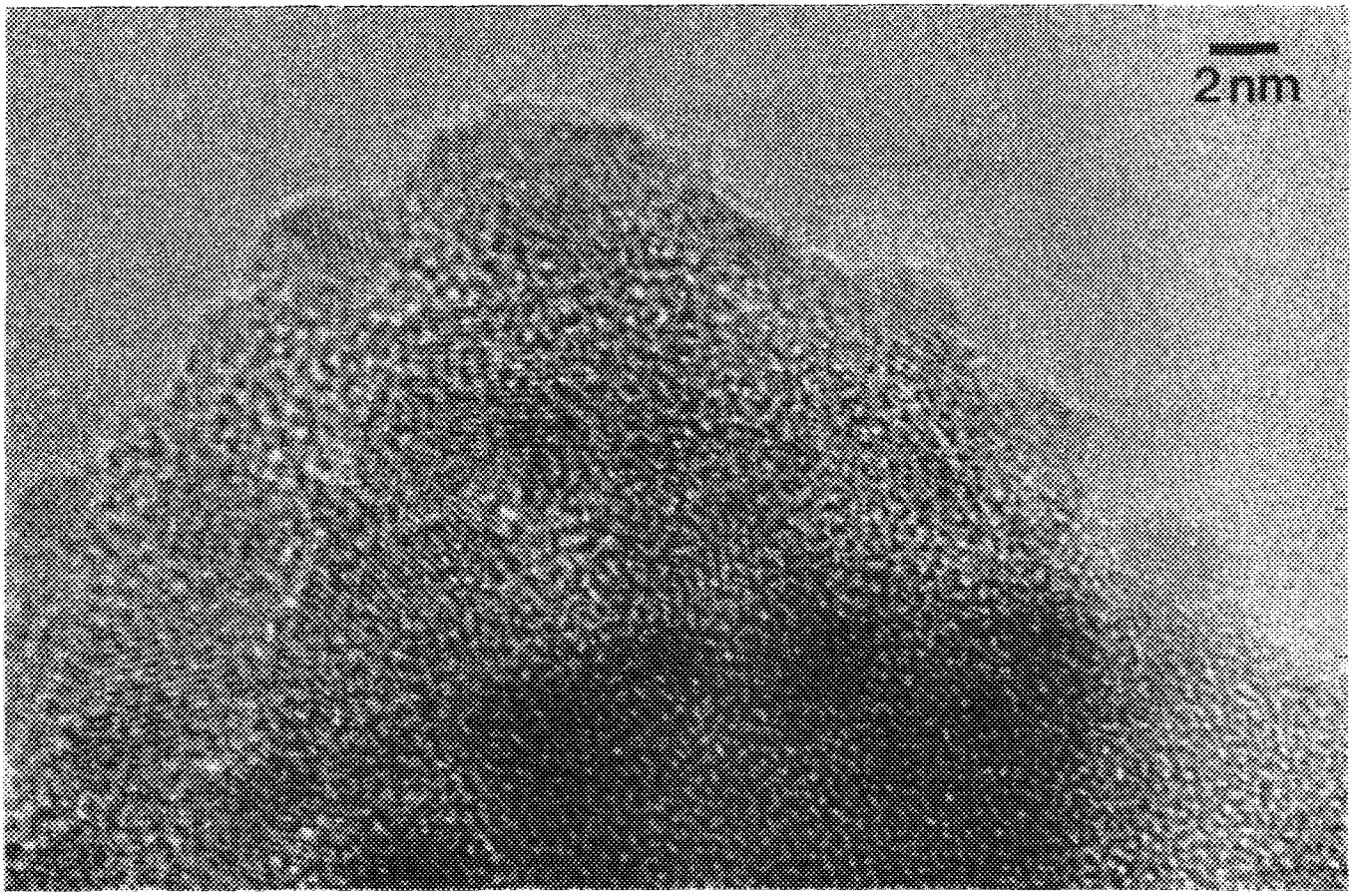

FIG. 11. HREM micrograph of Ni(4)NaY (ionex, dry sulf).

the most stable phase (28, 29). However, on supports which show a low interaction with the metal sulfide phase (e.g., carbon or silica) Ni_3S_2 is found to be present under reaction conditions (30, 31). On the other hand, on supports which have a strong interaction with the nickel sulfide mainly NiS is formed (17, 31). The interaction between the zeolite support and the nickel sulfide is probably very low, which results in the formation of Ni_3S_2. On the exterior of the zeolite particles very large nickel sulfide crystals are formed. These crystals exhibit properties close to that of bulk nickel sulfide and therefore they mainly consist of NiS.

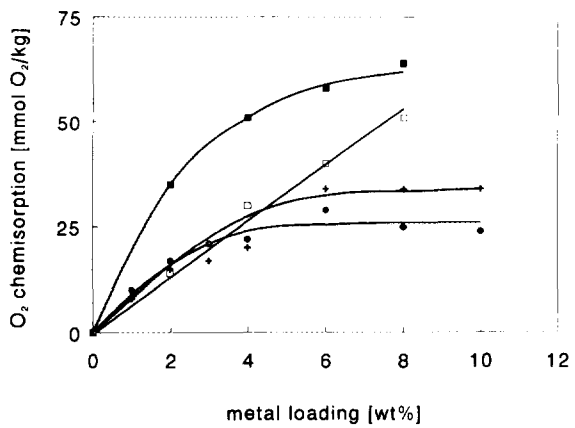

FIG. 12. Dynamic oxygen chemisorption (DOC) versus nickel loading: +, Ni(x)/NaY (imp); ●, Ni(x)/CaY (imp); □, Ni(x)NaY (ionex); ■, Ni(x)NaY (ionex, dry sulf) (conditions: see Figure 4).

The distribution of the nickel sulfide phase over the zeolite particles can be deduced from the results of the Xe adsorption and ^{129}Xe-NMR spectroscopy combined with those of the HREM–EDX experiments. For both Ni(4)/NaY (imp) and Ni(4)/CaY (imp) most of the nickel sulfide is located on the outside of the zeolite particles as large nickel sulfide clusters (up to 50 nm size). The part of the nickel sulfide which is located inside the zeolite pores is distributed inhomogeneously (20). Probably also in the zeolite pores large nickel sulfide particles have been formed, filling one or more adjacent supercages. Also Ni(4)NaY (ionex) contains nickel sulfide particles on the outside of the zeolite particles as large as on the impregnated catalysts. However, the amount of nickel sulfide located in the zeolite pores is somewhat higher. In addition, the distribution of this nickel sulfide is more homoge-

neous (20), resulting in smaller nickel sulfide clusters in the pores of the zeolite. Drying of the Ni(4)NaY (ionex) zeolite before sulfidation leads to catalysts with smaller nickel sulfide particles, both outside (HREM) and inside the zeolite pores (Xe adsorption and ^{129}Xe NMR).

These findings which are based on information obtained from Xe adsorption and ^{129}Xe-NMR measurements combined with HREM and EDX analysis are not completely in agreement with our earlier findings (20) which were exclusively based on Xe adsorption and ^{129}Xe-NMR results. At that time the latter results led us to conclude that in Ni(X)/NaY (imp) and Ni(x)NaY (ionex) catalysts nickel sulfide is mainly located inside the zeolite pores whereas from the additional information generated by HREM and EDX analysis the picture emerges that only a minor, though significant, part is located inside. The latter conclusion is consistent with the results reported by Cid *et al.* (6) who concluded from their XPS experiments on ion-exchanged NiNaY zeolites, that a certain Ni enrichment in the outer zeolite layers takes place after sulfidation, and this enrichment tends to be larger with increasing Ni exchange. In contrast herewith, Ezzamarty *et al.* (11) concluded also from XPS experiments that for ion-exchanged ultrastable Y zeolites Ni becomes better dispersed after sulfidation. This different behavior may have been caused by the different zeolite support, but it is also very well possible that the XPS results are misleading. Formation of large nickel sulfide particles at the outer surface of the zeolite particles can lead to lower Ni/Si ratios as measured by XPS, suggesting that the sulfide becomes better dispersed throughout the zeolite particle.

The reason for the differences in nickel sulfide distribution could be the preparation method itself. In the nonsulfided impregnated catalysts a large fraction of the nickel oxide is already located on the outside of the zeolite particles (HREM and EDX), although ^{129}Xe-NMR results suggests that also a fraction of the nickel phase is located inside the zeolite pores (20). Upon sulfidation this distribution will probably not change considerably, at the most even more nickel will move to the exterior of the zeolite particles. In the oxidic Ni(x)NaY (ionex) all nickel will be located inside the zeolite pores. It appears that upon sulfidation at 673 K a large part of the nickel migrates to the outside. Apparently, the location of the Ni in the zeolite pores before sulfidation is not decisive for the position of the nickel sulfide after sulfidation in these conditions. The migration of the nickel upon sulfidation in 10% H_2S/H_2 resembles the behavior observed for reduction under H_2 of Ni^{2+} ions in NiNaY zeolites (32–34). In this case sintering of the nickel metal on the exterior of the zeolite particles is found to take place. The physical cause for this phenomenon is the absence of nucleation sites in the supercages: upon reduction the Ni atoms leave the prisms and sodalite cages and traverse the supercages without encountering any nucleation site until they reach the outer surface (34). During sulfidation the nickel ions do not react with H_2, but with H_2S. However, the reason for the migration of the nickel species to the exterior surface may be the same.

On Ni(4)NaY (ionex, dry sulf) somewhat more nickel sulfide remained in the zeolite pores, and the sulfide particles are smaller compared to Ni(4)NaY (ionex). Apparently, the presence of water during the sulfidation process (sulfidation takes place between 350 K and 475 K, at which temperatures not all of the adsorbed water has been removed) improves the mobility and the sintering of the nickel sulfide. The fact that for the impregnated catalysts removal of the water does not lead to an increase in activity nor to an increase in dispersion of the nickel sulfide phase indicates that for these catalysts the distribution and dispersion of the sulfide phase is to a large extent determined by the distribution of the oxidic precursor species, and that the presence of water during the sulfidation process will not have more than a minor effect.

From the HREM–EDX, the Xe-adsorption, and ^{129}Xe-NMR results we can conclude that the distribution of the nickel sulfide phase on Ni(4)/NaY (imp), Ni(4)/CaY (imp) and Ni(4)NaY (ionex) is almost the same. Also the O_2 chemisorption measurements show that the nickel sulfide dispersions are comparable. In the ion-exchanged zeolites somewhat more nickel sulfide is present in the zeolite pores and it is possibly more uniformly distributed. However, apparently this difference is too small to manifest itself in the DOC results. The nickel sulfide dispersion in Ni(x)NaY (ionex, dry sulf) is clearly higher than in the other catalysts. This is in good agreement with the HREM results which show smaller nickel sulfide particles on the exterior of the zeolite particles, and with the ^{129}Xe-NMR results which indicate a more uniform distribution of the nickel sulfide particles inside the zeolite pores. This more homogeneous distribution will probably lead to more and smaller nickel sulfide particles, and consequently to a somewhat higher nickel sulfide surface area.

Using O/Ni ratios calculated from the DOC results, the dispersion of the zeolite supported nickel sulfide can be compared with the nickel sulfide dispersion in catalysts supported on Al_2O_3, SiO_2, or carbon. However, this should be done with caution since O_2 chemisorption is found to be corrosive, i.e., not limited to the outer surface (24, 35, 36). The O/Ni ratios for the zeolite-supported catalysts are low (Ni(4)/NaY (imp), 0.051; Ni(4)/CaY (imp), 0.053; Ni(4)NaY (ionex), 0.081; and Ni(4)NaY (ionex, dry sulf), 0.141). The highest O/Ni ratio observed is 0.193 for the Ni(2)NaY (ionex, dry sulf). This could indicate that the nickel sulfide dispersion is low compared with their Al_2O_3 and carbon-supported counterparts for which O/Ni ratios as high as 0.40 and 0.37, respectively, are found (23, 24). When supported on zeolite Y, nickel

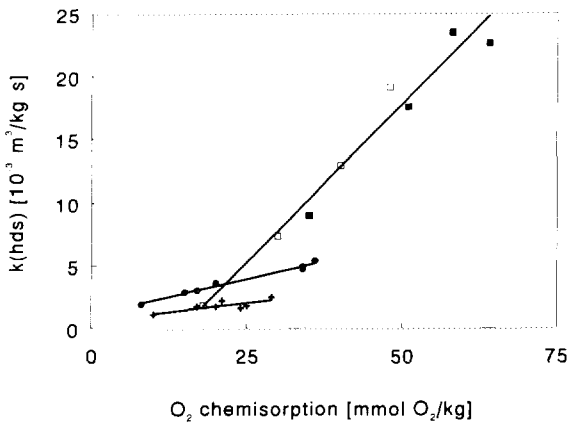

FIG. 13. Initial thiophene HDS activity as a function of the amount of oxygen chemisorbed: +, Ni(x)/NaY (imp); ●, Ni(x)/CaY (imp); □, Ni(x)NaY (ionex); ■, Ni(x)NaY (ionex, dry sulf) (conditions: see Fig. 5).

sulfide is most probably less well dispersed than when it is supported on Al_2O_3 or SiO_2. It is interesting to note that in spite of the lower nickel sulfide dispersion all zeolite-supported catalysts show thiophene HDS activities which are comparable to or higher than those of their counterparts supported on carbon or alumina (12, 23, 24). This strongly suggests that the nickel sulfide present in the zeolite-supported catalysts has a higher specific activity. The thiophene HDS activity per unit nickel sulfide surface area seems to be higher for the zeolite-supported catalysts than for the catalysts supported on Al_2O_3, SiO_2, or C. However, based on the DOC resuls, a quantitative comparison of dispersions and specific activities of the various supported nickel sulfide catalysts is not possible. Gosselink and Stork (37, 38) showed that such a comparison is only allowed within a narrowly defined group of catalysts, namely catalysts with the same metal sulfide phase and the same support.

In Fig. 13 the initial HDS activity of the zeolite Y-supported catalysts is plotted as a function of the amount of O_2 chemisorbed, in order to see whether the differences in catalytic activities can be explained by the differences in dispersion. All catalysts show a linear increase in activity with increasing nickel sulfide surface area. However, the slope of the line is different for the three types of catalyst and increases in the order Ni(x)/NaY (imp) < Ni(x)/CaY (imp) ≪ Ni(x)NaY (ionex). Although the nickel sulfide distribution and dispersion on both impregnated catalysts are nearly the same, the Ni(x)/CaY (imp) are more active, indicating that there is another factor influencing the activity of these catalysts. Both series of ion-exchanged catalysts, viz. Ni(x)NaY (ionex) and Ni(x)NaY (ionex, dry sulf), show the same linear relation between activity and nickel sulfide surface area. From this it can be concluded that the activity enhancement as a result of drying before sulfidation is completely caused by the improved nickel sulfide dispersion. The linear relationship between the activity and the nickel sulfide surface area of the ion-exchanged catalysts does not go through the origin. Apparently a part of the nickel sulfide chemisorbs O_2 but does not contribute to the catalytic activity. Also the linear relationship between the metal loading and the catalytic activity shown in Fig. 3 does not pass through the origin. A part of the nickel present on these catalysts is catalytically inactive. However, this nickel is sulfided and does chemisorb O_2. Further information about the structure and location of these nickel sulfide particles is needed to explain this phenomenon.

The different slopes between the three types of catalyst shown in Fig. 13 indicate that the HDS activity is not only determined by the nickel sulfide surface area but also by other factors such as (I) the interaction with the support, (II) the activity of the sulfide particles in the zeolite pores, or (III) the acidity of the support.

Re (I): As already discussed above, the interaction with the support can strongly influence the type of nickel sulfide which is formed. A strong interaction can lead to the formation of NiS (Al_2O_3 support), while a weak interaction results in the generation of Ni_3S_2 (SiO_2 or C supports) (31). The activity of the nickel sulfide phase will increase with the coordinative unsaturation of the Ni ion (39). As outlined by Burch and Collins (31), Ni_3S_2 will probably be more active than NiS. Hence sulfided Ni/Al_2O_3 catalysts show a significantly lower specific activity than sulfided Ni/SiO_2 or Ni/C catalysts. Zeolite Y will probably have a low interaction with the nickel sulfide phase. The nickel sulfide phase formed consists mainly of Ni_3S_2, and will therefore show specific thiophene HDS activities comparable with those of catalysts supported on carbon or silica.

Re (II): The nickel sulfide particles located in the zeolite pores may have a different activity from those located on the exterior of the zeolite particles, for instance because of the increased thiophene concentration in the micropores. Alternatively, the activity of the nickel sulfide clusters formed in the zeolite pores is higher due to their very small size. The nickel sulfide particles in the small zeolite pores will necessarily be very small and therefore highly disordered. This results in many coordinatively unsaturated sites, which could give a high specific HDS activity for the nickel sulfide particles located in the zeolite pores.

Re (III): Also the acidity of the zeolite support may influence the thiophene HDS activity of the nickel sulfide catalysts. Catalysts with Brønsted acid sites show a higher specific thiophene HDS activity than their NaY-supported counterparts. For a series of sulfided NiNaY (ionex) catalysts, Cid *et al.* (6) found the thiophene HDS activity to increase with increasing Ni loading and acidity. For other zeolite supports (ZSM-5, HNaY, HUSY) an increase in activity with growing acidity of the zeolite support is

found as well (40). The way in which acid sites influence the HDS activity is not yet clear. Possibly the acid sites improve the adsorption of thiophene on the zeolite, thus increasing the local thiophene concentration in the vicinity of the nickel sulfide active sites in the zeolite pores, which in turn results in an increased conversion. It is also possible that the acid sites have a direct effect on the thiophene HDS reaction itself. They might improve one step of the thiophene HDS reaction mechanism, as for instance the hydrogenation or breaking of the ring structure. Also in this case the effect will probably be stronger if more nickel sulfide is located in the zeolite pores, because this would facilitate the combined action of the sulfide and the acid sites. This point will be more extensively discussed elsewhere (40).

The observation that the catalysts with the highest amount of nickel sulfide in the zeolite pores (both the Ni(x)NaY (ionex) and the Ni(x)NaY (ionex, dry sulf) series) have very high initial activities supports the idea that especially nickel sulfide particles embedded in the zeolite pores are very active for thiophene HDS. Also the deactivation of these catalysts indicates that the nickel sulfide in the zeolite pores contributes significantly to the initial activity. Upon deactivation the pore system is almost completely blocked with coke (as shown by the BET measurements), while HREM revealed that most of the large nickel sulfide particles on the exterior can still be reached by thiophene. The low activity of the deactivated catalysts (see Figs. 1 and 4) indicates that the contribution of the nickel sulfide on the outside of the zeolite particles is relatively small compared to the contribution of the nickel sulfide located in the zeolite channels. Third, also the influence of the acid sites (which are mainly located in the zeolite pores) on the HDS activity and product selectivities suggests that the nickel sulfide particles in the zeolite pores contribute significantly to the thiophene HDS activity. However, to distinguish accurately between the activity of the nickel sulfide in the pores or on the exterior, model catalysts with nickel sulfide exclusively in the zeolite pores or on the outside should be developed.

CONCLUSIONS

Zeolite Y-supported nickel sulfide catalysts prepared by impregnation or by ion exchange show different catalytic behavior. The catalysts prepared by ion exchange are much more active for thiophene HDS than those prepared by impregnation, but they also show a considerably stronger deactivation.

All catalysts can be easily sulfided. Ni_3S_2 is preferentially formed, but also the formation of NiS is observed. On both impregnation and ion exchange type of catalysts a large part of the nickel sulfide phase is located on the outside of the zeolite particles. A smaller part is distributed through the pores of the zeolite. On the Ni(x) NaY (ionex) catalysts a higher and more homogeneously distributed amount of nickel sulfide is present in the zeolite pores.

Drying of the Ni(x)NaY (ionex) samples before sulfidation leads to smaller nickel sulfide particles, both in the zeolite pores and on the outside, resulting in a higher dispersion and consequently a higher activity.

The differences in activity between Ni(x)/NaY (imp), the Ni(x)/CaY (imp) and the Ni(x)NaY (ionex) are most probably not only caused by differences in nickel sulfide dispersion and distribution. Differences in acidity may also have some influence. A higher acidity might improve the thiophene HDS activity of the catalysts significantly. Moreover, also the very small nickel sulfide clusters located in the zeolite pores can have a high activity for thiophene HDS.

ACKNOWLEDGMENTS

These investigations have been supported by the Netherlands Foundation for Chemical Research (SON) with financial aid from the Netherlands Technology Foundation (STW). The authors thank Mrs. A. M. Elemans-Mehring and Mr. E. M. van Oers for conducting AAS and BET measurements and Mr. L. J. M. van de Ven for assistance with the ^{129}Xe-NMR experiments. TPS and HREM measurements were carried out at the Delft University of Technology with the assistance of Mr. J. P. Janssens and Mr. C. D. de Haan.

REFERENCES

1. Ward, J. W., *in* "Preparation of Catalysts III" (G. Poncelet, P. Grange and P. A. Jacobs, Eds.), p. 587. Elsevier, Amsterdam, 1983.
2. Marcelly, C., and Frank, J. P., *Stud. Surf. Sci. Catal.* **5,** 93 (1980).
3. Cid, R., Villasenor, J., Orellana, F., Fierro, J. L. G., and López Agudo, A., *Appl. Catal.* **18,** 357 (1985).
4. Cid, R., Orellana, F., and López Agudo, A., *Appl. Catal.* **32,** 327 (1987).
5. Fierro, J. L. G., Conesa, J. C., and López Agudo, A., *J. Catal.* **108,** 334 (1987).
6. Cid, R., Fierro, J. L. G., and López Agudo, A., *Zeolites* **10,** 95 (1990).
7. Davidova, N., Kovacheva, P., and Shopov, P., *Zeolites* **6,** 304 (1986).
8. Kovacheva, P., Davidova, N., and Novakova, J., *Zeolites* **11,** 54 (1991).
9. Laniecki, M., and Zmierczak, W., *in* "Zeolite Chemistry and Catalysis" (P. A. Jacobs *et al.*, Eds.), p. 331. Elsevier, Amsterdam, 1991.
10. Leglise, J., Janin, A., Lavalley, J. C., and Cornet, D., *J. Catal.* **114,** 388 (1988).
11. Ezzamarty, A., Catherine, E., Cornet, D., Hemidy, J. F., Janin, A., Lavalley, J. C., and Leglise, J., *in* "Zeolites, Facts, Figures, Future" (P. A. Jacobs and R. A. van Santen, Eds.), p. 1025. Elsevier, Amsterdam, 1989.
12. Welters, W. J. J., Korányi, T. I., de Beer, V. H. J., and van Santen, R. A., *in* "New Frontiers in Catalysis" (L. Guczi *et al.*, Eds.), p. 1931. Elsevier, Amsterdam, 1992.
13. Duchet, J. C., van Oers, E. M., de Beer, V. H. J., and Prins, R., *J. Catal.* **54,** 1 (1978).

14. Parillo, D. J., Adamo, A. T. Kokotailo, G. T., and Gorte, R. J., *Appl. Catal.* **67,** 107 (1990).
15. Pereira, C., and Gorte, R. J., *Appl. Catal.* **90,** 145 (1992).
16. Scheffer, B., Dekker, N. J. J., Mangnus, P. J., and Moulijn, J. A., *J. Catal.* **121,** 31 (1990).
17. Scheffer, B., Mangnus, P. J., and Moulijn, J. A., *J. Catal.* **121,** 18 (1990).
18. Fraissard, J., and Ito, T., *Zeolites* **8,** 350 (1988).
19. Ito, T., and Fraissard, J., *J. Chem. Phys.* **76,** 5225 (1982).
20. Korànyi, T. I., van de Ven, L. J. M., Welters, W. J. J., de Haan, J. W., de Beer, V. H. J., and van Santen, R. A., *Catal. Lett.* **17,** 105 (1993).
21. Bachelier, J., Duchet, J. C., and Cornet, D., *J. Phys. Chem.* **84,** 1925 (1980).
22. Bachelier, J., Tilliette, M. J., Duchet, J. C., and Cornet, D., *J. Catal.* **76,** 300 (1982).
23. Bachelier, J., Duchet, J. C., and Cornet, D., *J. Catal.* **87,** 283 (1984).
24. Bouwens, S. M. A. M., Barthe-Zahir, N., de Beer, V. H. J., and Prins, R., *J. Catal.* **131,** 326 (1991).
25. Karge, H. G., *in* "Catalysis and Adsorption by Zeolites" (G. Öhlmann *et al.*, Eds.), p. 133. Elsevier, Amsterdam, 1991.
26. Dwyer, J., *Stud. Surf. Sci. Catal.* **37,** 333 (1988).
27. Ito, T., and Fraissard, J., *J. Chem. Soc., Faraday Trans. 1,* **83,** 451 (1987).
28. Rosenquist, T., *J. Iron Steel Inst.* **176,** 37 (1954).
29. Mangnus, P. J., Ph. D. Thesis, University of Amsterdam, The Netherlands, 1989.
30. Louwers, S. P. A., and Prins, R., *J. Catal.* **133,** 94 (1992).
31. Burch, R., and Collins, A., *J. Catal.* **97,** 385 (1986).
32. Jacobs, P. A. Linart, J. P., Nijs, H., and Uytterhoeven, J. B., *J. Chem. Soc., Faraday Trans. 1,* **73,** 1745 (1977).
33. Schmidt, F. W., Bein, T., Ohlerich, U., and Jacobs, P. A., *in* "Proc. 6th International Zeolite Conference," Paper B-14. Butterworths, London, 1984.
34. Sachtler, W. M. H., Tzou, M. S., and Jiang, H. J., *Solid State Ionics* **26,** 71 (1988).
35. Zmierczack, W., MuraliDhar, G., and Massoth, F. E., *J. Catal.* **77,** 432 (1982).
36. Prins, R., de Beer, V. H. J., and Somorjai, G. A., *Catal. Rev. Sci. Eng.* **31,** 1 (1989).
37. Gosselink, J. W., and Stork, W. H. J., *Bull. Soc. Chim. Belg.* **96,** 901 (1987).
38. Gosselink, J. W., and Stork, W. H. J., *Appl. Catal.* **32,** 337 (1987).
39. Tanaka, K., and Okuhara, T., *Catal. Rev. Sci. Eng.* **15,** 249 (1977).
40. Welters, W. J. J., de Beer, V. H. J., and van Santen, R. A., to be published.